



Contents lists available at ScienceDirect

Advances in Engineering Software

journal homepage: www.elsevier.com/locate/advengsoft

Wave–current interactions over bottom with appreciable variations in both space and time

José Simão Antunes do Carmo

IMAR – University of Coimbra, Department of Civil Engineering, 3030-788 Coimbra, Portugal

ARTICLE INFO

Article history:

Received 12 June 2008

Received in revised form 30 January 2009

Accepted 17 July 2009

Available online xxx

Keywords:

Wave–wave and wave–current interactions

Mathematical formulations

Numerical models

Applications

ABSTRACT

In shallow water conditions, current and wave propagation cannot be simulated separately and then superposed linearly. In these conditions, in fact, the fluid dynamics of the wave and current motions and, as a consequence, the responses of the movable bed are significantly different from those expected for a linear superposition of a current with a sinusoidal wave. Thus, wave nonlinearity and the wave–current interaction effects become important factors that need to be considered. A model should be also able to reproduce the fluid dynamics under shallow water conditions over significant slopes and time–bed-level changes. This paper presents a 1DH mathematical formulation of a hydrodynamic model and its numerical solution. The model is able to reproduce all characteristic shallow water phenomena, including: (i) wave–wave and wave–current interaction effects; (ii) important ratios between the current and wave velocities; (iii) significant bed slopes and sudden time–bed-level changes, and (iv) friction stresses at the bottom and at the free surface. Different orders of mathematical approximations and appropriate application examples are also presented.

© 2009 Elsevier Ltd. All rights reserved.

1. Introduction

Knowledge of the flow characteristics associated with surface waves and currents, and their dependency on the bathymetry and coastal geometry, is of considerable importance when designing structures commonly found in the fluvial and coastal environment, like bridges, groynes and breakwaters. Such knowledge also helps to predict the modifications thereby introduced into local coastal dynamics behaviour and into the transport and deposition of sediments.

At the end of the 1970s linear models were used to simulate the refraction effect produced by the depth variation along the direction of the crest wave propagation and the diffraction effect produced by the gradient of the wave amplitude along its crest. However, as they are based on the linear theory, those models should not be utilized in shallow water conditions.

A number of factors have made it possible to employ increasingly complex mathematical models. Not only has our theoretical knowledge of the phenomena involved greatly improved, but numerical methods have been used more efficiently. The great strides made in computer technology, especially since the 1980s, improving information processing and enabling vast amounts of data to be stored, have meant that more mathematical models, of greater complexity, can be used, with fewer restrictions.

Monitoring this development, Saint-Venant type equations were frequently used in practical applications. However, as has been widely demonstrated, in shallow water conditions and for some types of waves, models based on a nondispersive theory, of which the Saint-Venant model is an example, are limited and are not usually able to compute satisfactory results over long periods of analysis [15,16].

Seabra-Santos et al. [16] define the domain of validity of the various possible approximations as linear dispersive, linear nondispersive, nonlinear nondispersive and nonlinear dispersive. For the last one they distinguish the cases of small relative amplitude and of large relative amplitude. They also present a comparison between experimental data and numerical results of the Korteweg–de Vries approximation. These data are here compared with the numerical results of a mathematical model developed in this work (Figs. 2 and 3).

It is widely accepted nowadays that for practical applications the combined gravity wave effects in shallow water conditions must be taken into account. In addition, the refraction and diffraction processes, the swelling, reflection and breaking waves, plus the wave–wave and wave–current interactions and the phenomena resulting from important sudden time–bed-level changes, all have to be considered, too.

Only nonlinear dispersive models of order σ^2 or greater, of the Boussinesq or Serre types, are able to reproduce effects other than the dispersive effects, including the nonlinearities resulting from wave–wave and wave–current interactions, and the waves

E-mail address: jsacarmo@dec.uc.pt

Nomenclature

a	characteristic wave amplitude	U	horizontal component of the velocity ($U = u + u_c$)
c_0	critical celerity ($c_0 = \sqrt{gh_0}$)	W	vertical component of the velocity; weighting function
g	gravitational acceleration	ε	dimensionless parameter ($\varepsilon = a/h_0$), which is a measure of nonlinearity
$h; h_0$	water depth; characteristic water depth	θ	parameter ($0.5 \leq \theta < 1$)
l	characteristic length	η	free-surface elevation
n	number of nodes of an element	ν	kinematic viscosity of the fluid
p	hydrodynamic pressure	ρ	density
r	auxiliary variable	σ	dimensionless shallow water parameter ($\sigma = h_0/l$), which is a measure of frequency dispersion
t	time	τ	stress tensor component
u, u_c	horizontal velocity components (subscript c denotes current)	τ_b, τ_s	stresses at the bottom and at the surface
x	horizontal coordinate	ξ	bed elevation
z	vertical coordinate	Δ	element; space and time increments ($\Delta x, \Delta t$)
N	interpolation (shape) function	Ω	vorticity component
R	Reynolds number; residual		

resulting from sudden time-bed-level changes that cause “tsunamis”, for example [3]. Submerged landslides in reservoirs and landslides on reservoir banks are other examples of important time-bed-level changes that must be taken into account in practical applications.

The dispersive properties of the conventional Boussinesq equation have been improved by modifying the dispersive terms [9] or using a reference velocity at a specified depth [11]. These techniques yield a set of equations whose linear dispersion relation can be adjusted such that the resulting intermediate-depth dispersion characteristics are close to those of linear wave theory. Liu [7] and Wei et al. [18] extended Nwogu’s approach to highly nonlinear waves, developing models that can not only be applied to intermediate water depth but are also capable of simulating wave propagation with strong nonlinear interaction. In general, these model equations contain accurate linear dispersion properties to $kh \approx 3$ (e.g. [11]).

The mathematical models described above use a quadratic polynomial approximation for the vertical flow distribution. More recent high-order models use fourth- and higher-order polynomial approximations. Gobbi et al. [6], using a fourth-order polynomial, developed a model with excellent linear dispersive properties up to $kh \approx 6$.

A different approach to obtaining a high-order depth-integrated model is followed by Lynett and Liu [8]. Instead of employing a high-order polynomial approximation for the vertical distribution of the flow field, two quadratic polynomials are used, matched at an interface that divides the water column into two layers. This approach leads to a set of model equations without the high-order spatial derivatives associated with high-order polynomial approximations. Through linear and nonlinear optimization of the interface and velocity evaluation locations, Lynett and Liu [8] show that the two-layer model exhibits accurate linear characteristics up to a $kh \approx 8$ and nonlinear accuracy to $kh \approx 6$. More recently, Zou and Fang [19] have presented alternative forms of the higher-order Boussinesq equations.

In this paper we use the general shallow water wave theory [10] to develop different mathematical approximations of orders 1 and 2 in σ^2 , which are nowadays the basis of the more important models in the ambit of hydrodynamics and sedimentary dynamics. In addition, three application examples of the order 2 in σ^2 approximation are presented. It is shown that this approximation is adequate to simulate wave \pm current interactions over a bottom with appreciable variations in both space and time.

The first example shows the model’s ability to reproduce wave-wave and wave-current interactions. The second is a real world

problem, with the objective of designing a submerged breakwater to protect a large coastal area. Finally, the third example shows the performance of the model for the propagation of a wave generated by a landslide moving into a reservoir.

2. Mathematical formulation

An adequate mathematical model for modelling wave propagation in shallow water conditions, with or without a current, may be obtained by vertically integrating the fundamental Fluid Mechanics equations relating to a three-dimensional viscous and incompressible fluid. This is done considering adequate dimensionless variables, with appropriate boundary conditions, and taking into account the fundamental hypothesis of shallow water.

In the context of the shallow water wave theory, different approximations are obtained by using a dimensionless form of the fundamental equations and grouping terms of different orders in accordance with their relative importance within the small parameter σ^2 . The dimensional forms of the equations are then obtained and solved numerically.

2.1. Fundamental equations

The fundamental equations of the fluid mechanics relating to a two-dimensional flow in the vertical plane and a quasi-irrotational flow of a viscous and incompressible fluid are written in Euler’s variables:

$$\begin{aligned} \frac{\partial U}{\partial x} + \frac{\partial W}{\partial z} &= 0 \\ \frac{\partial U}{\partial t} + U \frac{\partial U}{\partial x} + W \frac{\partial U}{\partial z} &= -\frac{1}{\rho} \frac{\partial p}{\partial x} + \frac{\partial \tau_{xx}}{\partial x} + \frac{\partial \tau_{xz}}{\partial z} \\ \frac{\partial W}{\partial t} + U \frac{\partial W}{\partial x} + W \frac{\partial W}{\partial z} &= -\frac{1}{\rho} \frac{\partial p}{\partial z} + \frac{\partial \tau_{zx}}{\partial x} + \frac{\partial \tau_{zz}}{\partial z} - g \\ \Omega &= \frac{1}{2} \left(\frac{\partial U}{\partial z} - \frac{\partial W}{\partial x} \right) \end{aligned} \quad (1)$$

where t is the time; U and W are the velocity components in the x and z directions, respectively, with the z axis pointing vertically upward (see Fig. 1); ρ is the density; g is the gravitational acceleration; p is the pressure; Ω is the vorticity component; and, τ_{xx} , τ_{xz} and τ_{zz} are the tensor elements of the viscous stresses, which, according to the Navier hypotheses, are defined as:

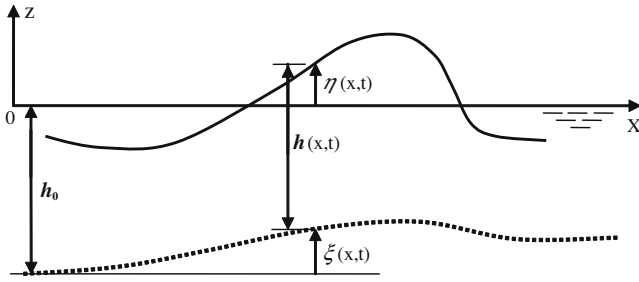


Fig. 1. Notations.

$$\tau_{xx} = 2\nu \frac{\partial U}{\partial x}; \quad \tau_{xz} = \nu \left(\frac{\partial W}{\partial x} + \frac{\partial U}{\partial z} \right); \quad \tau_{zz} = 2\nu \frac{\partial W}{\partial z} \quad (2)$$

in which ν is the kinematic viscosity.

2.2. Boundary conditions

Consider the notations presented in Fig. 1.

The usual boundary conditions for the free surface flow problem are:

- At the surface, $z = \eta(x, t)$
 - Kinematic condition: $\frac{\partial \eta}{\partial t} + U \frac{\partial \eta}{\partial x} = W$
 - Dynamical conditions: $-\tau_{xx} \frac{\partial \eta}{\partial x} + \tau_{xz} = \tau_s(\eta);$ (3)
 - $\frac{p}{\rho} + \tau_{zx} \frac{\partial \eta}{\partial x} - \tau_{zz} = 0$

- At the bottom, $z = -h_0 + \zeta(x, t)$
 - Kinematic condition: $\frac{\partial \zeta}{\partial t} + U \frac{\partial \zeta}{\partial x} = W$ (4)
 - Dynamical condition: $-\tau_{xx} \frac{\partial \zeta}{\partial x} + \tau_{xz} = \tau_b(\zeta)$

2.3. Equations in dimensionless variables

Proceeding with the following suitable dimensionless variables:

$$\begin{aligned} x^* &= \frac{x}{l}; & z^* &= \frac{z}{h_0}; & \eta^* &= \frac{\eta}{a}; & \zeta^* &= \frac{\zeta}{h_0} \\ t^* &= \sqrt{gh_0} \frac{t}{l} = c_0 \frac{t}{l}; & u_c^* &= \frac{u_c}{\sqrt{gh_0}} = \frac{u_c}{c_0} \\ u^* &= \frac{u}{a\sqrt{g/h_0}} = \frac{uh_0}{ac_0}; & W^* &= \frac{Wl}{ah_0\sqrt{g/h_0}} = \frac{Wl}{ac_0} \\ p^* &= \frac{p}{\rho gh_0}; & \tau_{xx}^* &= \frac{\tau_{xx}}{gh_0}; & \tau_{xz}^* &= \frac{\tau_{xz}}{gh_0}; & \tau_{zz}^* &= \frac{\tau_{zz}}{gh_0} \end{aligned} \quad (5)$$

the small non-dimensional parameters $\varepsilon = a/h_0$ and $\sigma = h_0/l$ are defined, where h_0 , l and a represent, respectively, a characteristic depth, a characteristic length and a characteristic wave amplitude, and c_0 is the critical celerity ($c_0 = \sqrt{gh_0}$).

In these conditions, taking $U = u + u_c$ a dimensionless velocity is written $U^* = u^* + (1/\varepsilon)u_c^*$ and the complete set of governing Eqs. (1) and (2), as well as the boundary conditions (3) and (4), are now written as follows:

(I) Fundamental equations

$$\begin{aligned} \text{(a)} \quad & \frac{\partial U^*}{\partial x^*} + \frac{\partial W^*}{\partial z^*} = 0 \\ \text{(b)} \quad & \varepsilon \sigma \frac{\partial U^*}{\partial t^*} + \varepsilon^2 \sigma U^* \frac{\partial U^*}{\partial x^*} + \varepsilon^2 \sigma W^* \frac{\partial U^*}{\partial z^*} \\ & = -\sigma \frac{\partial p^*}{\partial x^*} + \sigma \frac{\partial \tau_{xx}^*}{\partial x^*} + \frac{\partial \tau_{xz}^*}{\partial z^*} \end{aligned}$$

$$\begin{aligned} \text{(c)} \quad & \varepsilon \sigma^2 \frac{\partial W^*}{\partial t^*} + \varepsilon^2 \sigma^2 U^* \frac{\partial W^*}{\partial x^*} + \varepsilon^2 \sigma^2 W^* \frac{\partial W^*}{\partial z^*} \\ & = -\frac{\partial p^*}{\partial z^*} + \sigma \frac{\partial \tau_{zx}^*}{\partial x^*} + \frac{\partial \tau_{zz}^*}{\partial z^*} - 1 \\ \text{(d)} \quad & \Omega^* = \frac{1}{2} \left(\frac{\partial U^*}{\partial z^*} - \sigma^2 \frac{\partial W^*}{\partial x^*} \right) \end{aligned}$$

(II) Boundary conditions

- At the surface, $z^* = \varepsilon \eta^*(x^*, t^*)$

$$\begin{aligned} \frac{\partial \eta^*}{\partial t^*} + \varepsilon U^* \frac{\partial \eta^*}{\partial x^*} &= W^* \\ -\varepsilon \sigma \tau_{xx}^* \frac{\partial \eta^*}{\partial x^*} + \tau_{xz}^* &= \tau_s^*(\varepsilon \eta^*) \\ p^* + \varepsilon \sigma \tau_{zx}^* \frac{\partial \eta^*}{\partial x^*} - \tau_{zz}^* &= 0 \end{aligned} \quad (7)$$
- At the bottom, $z^* = -1 + \zeta^*(x^*, t^*)$

$$\begin{aligned} \frac{1}{\varepsilon} \frac{\partial \zeta^*}{\partial t^*} + U^* \frac{\partial \zeta^*}{\partial x^*} &= W^* \\ -\sigma \tau_{xx}^* \frac{\partial \zeta^*}{\partial x^*} + \tau_{xz}^* &= \tau_b^*(-1 + \zeta^*) \end{aligned} \quad (8)$$

where the dimensionless tensor elements of the viscous stresses are given by:

$$\begin{aligned} \tau_{xx}^* &= 2 \frac{\varepsilon \sigma}{R} \frac{\partial U^*}{\partial x^*}; & \tau_{zz}^* &= 2 \frac{\varepsilon \sigma}{R} \frac{\partial W^*}{\partial z^*} \\ \tau_{xz}^* &= \tau_{zx}^* = \frac{\varepsilon}{R} \left(\sigma^2 \frac{\partial W^*}{\partial x^*} + \frac{\partial U^*}{\partial z^*} \right) \end{aligned} \quad (9)$$

with the Reynolds number $R = \frac{h_0 c_0}{\nu}$.

For convenience, we proceed without the asterisk (*).

2.4. Formulation of the continuity equation

Taking into account the Leibniz rule, Eq. (6a) may be integrated between $(-1 + \zeta)$ and $(\varepsilon \eta)$ to give:

$$W|_{\varepsilon \eta} - W|_{-1+\zeta} = -\frac{\partial}{\partial x} \int_{-1+\zeta}^{\varepsilon \eta} U dz + \varepsilon U|_{\varepsilon \eta} \frac{\partial \eta}{\partial x} - U|_{-1+\zeta} \frac{\partial \zeta}{\partial x} \quad (10)$$

Taking into account the kinematic boundary conditions at the surface $(\varepsilon \eta)$ and at the bottom, as well as the mean horizontal component of the velocity field, defined as $\bar{U} = \frac{1}{1-\varepsilon+\varepsilon \eta} \int_{-1+\zeta}^{\varepsilon \eta} U dz$, Eq. (10) allows us to obtain the continuity equation in dimensionless variables:

$$\frac{\partial}{\partial t} \left(\eta - \frac{\zeta}{\varepsilon} \right) + \frac{\partial}{\partial x} [(1 - \zeta + \varepsilon \eta) \bar{U}] = 0 \quad (11)$$

2.5. Formulation of the momentum equation

This equation is deduced accepting the fundamental hypothesis of the shallow water wave theory ($\sigma \ll 1$) and assuming that the ratio of a typical measure of the wave height a to the mean water depth h_0 is small, i.e. with the relative elevation of the surface due to the waves ($\varepsilon = a/h_0$) having a value close to the square of the relative depth ($\sigma = h_0/l$), which means that $0(\varepsilon) = 0(\sigma^2)$.

2.5.1. Vertical component of the velocity, W

Accepting small vorticity [$\Omega \cong O(\sigma^4)$] we can write,

$$\frac{\partial U}{\partial z} = \sigma^2 \frac{\partial W}{\partial x} + O(\sigma^4) \quad (12)$$

Let us now consider $\bar{U}(x, t)$ the horizontal velocity component at the surface ($z = 0$). Thus, from Eq. (12), the U -velocity component becomes:

$$U(x, z, t) = \bar{U}(x, t) + O(\sigma^2) \quad (13)$$

Integrating Eq. (6a) between $(-1 + \xi)$ and (z) , and substituting the equation thus obtained into (12) it follows that:

$$\frac{\partial U}{\partial z} = -\sigma^2 \frac{\partial}{\partial x} \int_{-1+\xi}^z \frac{\partial U}{\partial x} dz + \sigma^2 \frac{\partial}{\partial x} \left(\frac{1}{\varepsilon} \frac{\partial \xi}{\partial t} + U \frac{\partial \xi}{\partial x} \right) + O(\sigma^4) \quad (14)$$

From this Eq. (14), taking into account (13) and considering the kinematic boundary condition at the bottom, the vertical velocity component becomes, after integration:

$$W = -(1 - \xi + z) \frac{\partial \bar{U}}{\partial x} + \frac{1}{\varepsilon} \frac{\partial \xi}{\partial t} + \frac{\partial \xi}{\partial x} \bar{U} + O(\sigma^2) \quad (15)$$

2.5.2. Pressure

Incorporating Eq. (15) into Eq. (6c), the following expression (16) for the vertical pressure gradient is obtained:

$$\begin{aligned} \frac{\partial p}{\partial z} = & -1 - \sigma^2 \frac{\partial^2 \xi}{\partial t^2} - \varepsilon \sigma^2 \frac{\partial \xi}{\partial x} \frac{\partial \bar{U}}{\partial t} - 2\varepsilon \sigma^2 \frac{\partial^2 \xi}{\partial x \partial t} \bar{U} + \varepsilon \sigma^2 (1 - \xi + z) \frac{\partial^2 \bar{U}}{\partial x \partial t} \\ & + \varepsilon \sigma^2 (1 - \xi + z) u_c \frac{\partial^2 \bar{U}}{\partial x^2} - \varepsilon \sigma^2 \frac{\partial \xi}{\partial x} u_c \frac{\partial \bar{U}}{\partial x} + \varepsilon \sigma^2 (1 - \xi + z) \frac{\partial^2 u_c \bar{U}}{\partial x^2} \\ & - \varepsilon \sigma^2 \frac{\partial \xi}{\partial x} \frac{\partial u_c \bar{U}}{\partial x} - \varepsilon \sigma^2 \frac{\partial^2 \xi}{\partial x^2} u_c \bar{U} - \varepsilon \sigma^2 (1 - \xi + z) \frac{\partial u_c \bar{U}}{\partial x} \\ & + \sigma \frac{\partial \tau_{zx}}{\partial x} + \frac{\partial \tau_{zz}}{\partial z} + O(\varepsilon^2 \sigma^2, \varepsilon \sigma^4) \end{aligned} \quad (16)$$

2.5.3. Integration of Eq. (6b)

Let us now consider Eq. (6b). The left-hand side of this equation may be integrated between $(-1 + \xi)$ and $(\varepsilon \eta)$, taking into account the Leibniz rule, the continuity Eq. (6a) and the kinematic boundary conditions. In terms of the mean values of the horizontal velocity component, the left-hand side is written:

$$M1x = \varepsilon \sigma (1 - \xi + \varepsilon \eta) \frac{\partial \bar{U}}{\partial t} + \varepsilon^2 \sigma (1 - \xi + \varepsilon \eta) \bar{U} \frac{\partial \bar{U}}{\partial x} + O(\varepsilon^2 \sigma^2, \varepsilon^3 \sigma) \quad (17)$$

In the same way, the right-hand side of Eq. (6b) may be integrated as follows:

$$\begin{aligned} M2x = & -\sigma \int_{-1+\xi}^{\varepsilon \eta} \frac{\partial p}{\partial x} dz + \sigma \frac{\partial}{\partial x} \int_{-1+\xi}^{\varepsilon \eta} \tau_{xx} dz \\ & + \left(-\varepsilon \sigma \tau_{xx} \frac{\partial \eta}{\partial x} + \tau_{xz} \right)_{\varepsilon \eta} + \left(\sigma \tau_{xx} \frac{\partial \xi}{\partial x} - \tau_{xz} \right)_{-1+\xi} \end{aligned} \quad (18)$$

Integrating Eq. (16) between (z) and $(\varepsilon \eta)$, taking into account Eqs. (7) and (9), an expression for the pressure $p(z)$ is written. After substitution of the equation obtained for the pressure $p(z)$ into Eq. (18), making use of Eqs. (7) and (8), and taking mean quantities of the horizontal component of the velocity field, the right-hand side of Eq. (18) is easily obtained after simple mathematical manipulations.

Thus, with the continuity Eqs. (11), (17) and (18) allow us to write the following equation system (19), which constitutes an adequate mathematical model to reproduce the flow in shallow water conditions, taking into account: (i) wave-wave and wave-current interaction effects; (ii) important ratios between the current and the wave velocities; (iii) appreciable bottom slopes and sudden time-bed-level changes; and (iv) friction stresses at the bottom and at the free surface. In dimensionless variables, the complete set of equations is written:

$$\begin{aligned} \frac{\partial}{\partial t} \left(\eta - \frac{\xi}{\varepsilon} \right) + \frac{\partial}{\partial x} [(1 - \xi + \varepsilon \eta) \bar{U}] = & 0 \\ \frac{\partial \bar{U}}{\partial t} + \varepsilon \bar{U} \frac{\partial \bar{U}}{\partial x} + \frac{\partial \eta}{\partial x} + \sigma^2 \left\{ \frac{(1 - \xi + \varepsilon \eta)}{2\varepsilon} \frac{\partial^3 \xi}{\partial x \partial t^2} \right. \\ & - \frac{(1 - \xi)^2}{3} \frac{\partial^3 \bar{U}}{\partial x^2 \partial t} + \frac{(1 - \xi)}{2} \frac{\partial \xi}{\partial x} \frac{\partial^2 \bar{U}}{\partial x \partial t} \\ & + \frac{\partial \eta}{\partial x} \frac{\partial^2 \xi}{\partial t^2} + \frac{(1 - \xi)}{2} \frac{\partial}{\partial x} \left(\frac{\partial \xi}{\partial x} \frac{\partial \bar{U}}{\partial t} + 2 \frac{\partial^2 \xi}{\partial x \partial t} \bar{U} \right) \\ & - \frac{(1 - \xi)^2}{3} \frac{\partial}{\partial x} \left(u_c \frac{\partial^2 \bar{U}}{\partial x^2} + \frac{\partial^2 u_c \bar{U}}{\partial x^2} - \frac{\partial u_c}{\partial x} \frac{\partial \bar{U}}{\partial x} \right) \\ & + \frac{(1 - \xi)}{2} \frac{\partial \xi}{\partial x} \left(u_c \frac{\partial^2 \bar{U}}{\partial x^2} + \frac{\partial^2 u_c \bar{U}}{\partial x^2} - \frac{\partial u_c}{\partial x} \frac{\partial \bar{U}}{\partial x} \right) \\ & + \frac{(1 - \xi)}{2} \frac{\partial}{\partial x} \left(\frac{\partial \xi}{\partial x} u_c \frac{\partial \bar{U}}{\partial x} + \frac{\partial \xi}{\partial x} \frac{\partial u_c \bar{U}}{\partial x} \right) \\ & \left. + \frac{(1 - \xi)}{2} \frac{\partial}{\partial x} \left(\frac{\partial^2 \xi}{\partial x^2} u_c \bar{U} \right) \right\} - \frac{\sigma}{R} \frac{\partial^2 \bar{U}}{\partial x^2} \\ & - \frac{\tau(\varepsilon \eta) - \tau(-1 + \xi)}{\varepsilon \sigma (1 - \xi + \varepsilon \eta)} = O\left(\varepsilon \sigma, \sigma^3, \frac{\sigma^2}{R}\right) \end{aligned} \quad (19)$$

In dimensional variables, without a bar on the variables, those approximations are written as follows:

(A) – Order 2 in σ^2 (wave ± current, over bottom with appreciable variations in both space and time)

$$\begin{aligned} \frac{\partial h}{\partial t} + \frac{\partial(hU)}{\partial x} = & 0 \\ \frac{\partial U}{\partial t} + U \frac{\partial U}{\partial x} + g \frac{\partial \eta}{\partial x} + \frac{h_0 - \xi + \eta}{2} \frac{\partial^3 \xi}{\partial x \partial t^2} \\ & - \frac{(h_0 - \xi)^2}{3} \frac{\partial^3 U}{\partial x^2 \partial t} + \frac{(h_0 - \xi)}{2} \frac{\partial \xi}{\partial x} \frac{\partial^2 U}{\partial x \partial t} \\ & + \frac{\partial \eta}{\partial x} \frac{\partial^2 \xi}{\partial t^2} + \frac{(h_0 - \xi)}{2} \frac{\partial}{\partial x} \left(\frac{\partial \xi}{\partial x} \frac{\partial U}{\partial t} + 2 \frac{\partial^2 \xi}{\partial x \partial t} U \right) \\ & - \frac{(h_0 - \xi)^2}{3} \frac{\partial}{\partial x} \left(u_c \frac{\partial^2 U}{\partial x^2} + \frac{\partial^2 u_c U}{\partial x^2} - \frac{\partial u_c}{\partial x} \frac{\partial U}{\partial x} \right) \\ & + \frac{(h_0 - \xi)}{2} \frac{\partial \xi}{\partial x} \left(u_c \frac{\partial^2 U}{\partial x^2} + \frac{\partial^2 u_c U}{\partial x^2} - \frac{\partial u_c}{\partial x} \frac{\partial U}{\partial x} \right) \\ & + \frac{(h_0 - \xi)}{2} \frac{\partial}{\partial x} \left(\frac{\partial \xi}{\partial x} u_c \frac{\partial U}{\partial x} + \frac{\partial \xi}{\partial x} \frac{\partial u_c U}{\partial x} \right) \\ & + \frac{(1 - \xi)}{2} \frac{\partial}{\partial x} \left(\frac{\partial^2 \xi}{\partial x^2} u_c U \right) - v \frac{\partial^2 U}{\partial x^2} - \frac{\tau_s - \tau_b}{h} = 0 \end{aligned} \quad (20)$$

(B) – Order 2 in σ^2 (wave propagation over bottom with appreciable variations in both space and time)

$$\begin{aligned} \frac{\partial h}{\partial t} + \frac{\partial(hU)}{\partial x} = & 0 \\ \frac{\partial U}{\partial t} + U \frac{\partial U}{\partial x} + \left(g + \frac{\partial^2 \xi}{\partial t^2} \right) \frac{\partial \eta}{\partial x} + \frac{h}{2} \frac{\partial^3 \xi}{\partial x \partial t^2} \\ & - \frac{(h_0 - \xi)^2}{3} \frac{\partial^3 U}{\partial x^2 \partial t} + \frac{(h_0 - \xi)}{2} \frac{\partial \xi}{\partial x} \frac{\partial^2 U}{\partial x \partial t} \\ & + \frac{(h_0 - \xi)}{2} \frac{\partial}{\partial x} \left(\frac{\partial \xi}{\partial x} \frac{\partial U}{\partial t} + 2 \frac{\partial^2 \xi}{\partial x \partial t} U \right) \\ & - v \frac{\partial^2 U}{\partial x^2} - \frac{\tau_s - \tau_b}{h} = 0 \end{aligned} \quad (21)$$

(C) – Order 2 in σ^2 (wave propagation over bottom with appreciable variations in space)

$$\begin{aligned} \frac{\partial h}{\partial t} + \frac{\partial(hU)}{\partial x} &= 0 \\ \frac{\partial U}{\partial t} + U \frac{\partial U}{\partial x} + g \frac{\partial \eta}{\partial x} - \frac{(h_0 - \xi)^2}{3} \frac{\partial^3 U}{\partial x^2 \partial t} \\ &+ (h_0 - \xi) \frac{\partial \xi}{\partial x} \frac{\partial^2 U}{\partial x \partial t} + \frac{(h_0 - \xi)}{2} \frac{\partial^2 \xi}{\partial x^2} \frac{\partial U}{\partial t} \\ &- v \frac{\partial^2 U}{\partial x^2} - \frac{\tau_s - \tau_b}{h} = 0 \end{aligned} \quad (22)$$

(D) – Order 1 in σ^2 (Saint-Venant or shallow-water equations)

$$\begin{aligned} \frac{\partial h}{\partial t} + \frac{\partial(hU)}{\partial x} &= 0 \\ \frac{\partial U}{\partial t} + U \frac{\partial U}{\partial x} + g \frac{\partial \eta}{\partial x} - v \frac{\partial^2 U}{\partial x^2} - \frac{\tau_s - \tau_b}{h} &= 0 \end{aligned} \quad (23)$$

3. Numerical model

3.1. Equivalent equation system

Let us consider the equation system (20) (wave \pm current, over irregular and important time variable bottoms). Grouping terms containing U -derivatives in time in this system of equations, we can re-write an equivalent form of system (20) in the following form:

$$\begin{aligned} \frac{\partial h}{\partial t} + h \frac{\partial U}{\partial x} + U \frac{\partial h}{\partial x} &= 0 \\ \frac{\partial r}{\partial t} &= -U \frac{\partial U}{\partial x} - \left(g + \frac{\partial^2 \xi}{\partial t^2} \right) \frac{\partial(h + \xi)}{\partial x} - \frac{h}{2} \frac{\partial^3 \xi}{\partial x \partial t^2} \\ &- (h_0 - \xi) \frac{\partial}{\partial x} \left(\frac{\partial^2 \xi}{\partial x \partial t} U \right) - \frac{\partial}{\partial t} \frac{(h_0 - \xi)^2}{3} \frac{\partial^2 U}{\partial x^2} \\ &+ \frac{\partial}{\partial t} \left[(h_0 - \xi) \frac{\partial \xi}{\partial x} \frac{\partial U}{\partial x} + \frac{\partial}{\partial t} \left[\frac{(h_0 - \xi)}{2} \frac{\partial^2 \xi}{\partial x^2} \right] U \right] \\ &+ \frac{(h_0 - \xi)^2}{3} \frac{\partial}{\partial x} \left(u_c \frac{\partial^2 U}{\partial x^2} + \frac{\partial^2 u_c}{\partial x^2} U - \frac{\partial u_c}{\partial x} \frac{\partial U}{\partial x} \right) \\ &- \frac{(h_0 - \xi)}{2} \frac{\partial \xi}{\partial x} \left(u_c \frac{\partial^2 U}{\partial x^2} + \frac{\partial^2 u_c}{\partial x^2} U - \frac{\partial u_c}{\partial x} \frac{\partial U}{\partial x} \right) \\ &- \frac{(h_0 - \xi)}{2} \frac{\partial}{\partial x} \left(\frac{\partial \xi}{\partial x} u_c \frac{\partial U}{\partial x} + \frac{\partial \xi}{\partial x} \frac{\partial u_c}{\partial x} U \right) \\ &- \frac{(1 - \xi)}{2} \frac{\partial}{\partial x} \left(\frac{\partial^2 \xi}{\partial x^2} u_c U \right) + v \frac{\partial^2 U}{\partial x^2} + \frac{\tau_s - \tau_b}{h} \\ U - \frac{(h_0 - \xi)^2}{3} \frac{\partial^2 U}{\partial x^2} + (h_0 - \xi) \frac{\partial \xi}{\partial x} \frac{\partial U}{\partial x} + \frac{h_0 - \xi}{2} \frac{\partial^2 \xi}{\partial x^2} U &= r \end{aligned} \quad (24)$$

It is easy to show that after substituting the third equation in the second one of system (24), we again find the final system of Eq. (20).

To compute the solution of equation system (20) (values of the variables h and U at time $t + \Delta t$) we can use a numerical procedure based on the following numerical scheme, itself based on the last equation system (24), for the variables h, r and U [1,2]:

- (1) The first equation allows us to predict the values of variable $h(h_p^{t+\Delta t})$ utilizing a semi-implicit scheme, considering the known values of h and U at time t in the whole domain.
- (2) The second equation allows the explicit prediction of the values of variable $r(r_p^{t+\Delta t})$, considering the values of $h^{t+\theta \Delta t} = (1 - \theta)h^t + \theta h_p^{t+\Delta t}$, U^t and r^t , known for the whole domain.

- (3) The third equation allows us to obtain the values of variable U at time $t + \Delta t(U^{t+\Delta t})$ utilizing a semi-implicit scheme, considering the predicted values of $r(r_p^{t+\Delta t})$ in the whole domain.
- (4) The first equation allows us to compute the depth h at time $t + \Delta t(h^{t+\Delta t})$, taking into account the values of variables h^t and $U^{t+\theta \Delta t} = (1 - \theta)U^t + \theta U^{t+\Delta t}$ known for the whole domain.
- (5) The second equation allows us to compute the values of variable r at time $t + \Delta t(r^{t+\Delta t})$, taking into account the values of variables r^t , $h^{t+\theta \Delta t} = (1 - \theta)h^t + \theta h^{t+\Delta t}$ and $U^{t+\theta \Delta t} = (1 - \theta)U^t + \theta U^{t+\Delta t}$ known for the whole domain.

3.2. Finite differences method

Schematically, in finite differences form, the equivalent system of Eq. (24), for variables h, r and U , may be written in the following form:

$$\begin{aligned} &- \frac{U_i^n}{4\Delta x} h_{i-1}^{n+1} + \left[\frac{1}{\Delta t} + \frac{1}{2} \left(\frac{\partial U}{\partial x} \right)_i \right] h_i^{n+1} + \frac{U_i^n}{4\Delta x} h_{i+1}^{n+1} \\ &= \left[\frac{1}{\Delta t} - \frac{1}{2} \left(\frac{\partial U}{\partial x} \right)_i \right] h_i^n - U_i^n \frac{1}{2} \left(\frac{\partial h}{\partial x} \right)_i \\ h_i^{n+\theta} &= (1 - \theta)h_i^n + \theta h_i^{n+1} \\ r_i^{n+1} &= r_i^n - \left[U \frac{\partial U}{\partial x} \right]_i^n \Delta t \\ &- \left[\left(g + \frac{\partial^2 \xi}{\partial t^2} \right) \frac{\partial(h + \xi)}{\partial x} + \frac{h}{2} \frac{\partial^3 \xi}{\partial x \partial t^2} \right]_i^{n+\theta} \Delta t \\ &- \left[(h_0 - \xi) \frac{\partial}{\partial x} \left(\frac{\partial^2 \xi}{\partial x \partial t} U \right) + \frac{\partial}{\partial t} \frac{(h_0 - \xi)^2}{3} \frac{\partial^2 U}{\partial x^2} \right]_i^n \Delta t \\ &+ \left[\frac{\partial}{\partial t} \left[(h_0 - \xi) \frac{\partial \xi}{\partial x} \frac{\partial U}{\partial x} + \frac{\partial}{\partial t} \left[\frac{(h_0 - \xi)}{2} \frac{\partial^2 \xi}{\partial x^2} \right] U \right] \right]_i^n \Delta t \\ &+ \left[\frac{(h_0 - \xi)^2}{3} \frac{\partial}{\partial x} \left(u_c \frac{\partial^2 U}{\partial x^2} + \frac{\partial^2 u_c}{\partial x^2} U - \frac{\partial u_c}{\partial x} \frac{\partial U}{\partial x} \right) \right]_i^n \Delta t \\ &- \left[\frac{(h_0 - \xi)}{2} \frac{\partial \xi}{\partial x} \left(u_c \frac{\partial^2 U}{\partial x^2} + \frac{\partial^2 u_c}{\partial x^2} U - \frac{\partial u_c}{\partial x} \frac{\partial U}{\partial x} \right) \right]_i^n \Delta t \\ &- \left[\frac{(h_0 - \xi)}{2} \frac{\partial}{\partial x} \left(\frac{\partial \xi}{\partial x} u_c \frac{\partial U}{\partial x} + \frac{\partial \xi}{\partial x} \frac{\partial u_c}{\partial x} U \right) \right]_i^n \Delta t \\ &- \left[\frac{(1 - \xi)}{2} \frac{\partial}{\partial x} \left(\frac{\partial^2 \xi}{\partial x^2} u_c U \right) - v \frac{\partial^2 U}{\partial x^2} \right]_i^n \Delta t + \left(\frac{\tau_s - \tau_b}{h} \right)_i^{n+\theta} \Delta t \\ &\left[- \frac{(h_0 - \xi)^2}{3(\Delta x)^2} + \frac{(h_0 - \xi)}{2\Delta x} \frac{\partial(h_0 - \xi)}{\partial x} \right]_i^n U_{i-1}^{n+1} \\ &+ \left[1 + \frac{2(h_0 - \xi)^2}{3(\Delta x)^2} - \frac{h_0 - \xi}{2} \frac{\partial^2(h_0 - \xi)}{\partial x^2} \right]_i^n U_i^{n+1} \\ &- \left[\frac{(h_0 - \xi)^2}{3(\Delta x)^2} + \frac{(h_0 - \xi)}{2\Delta x} \frac{\partial(h_0 - \xi)}{\partial x} \right]_i^n U_{i+1}^{n+1} = r_i^{n+1} \\ U_i^{n+\theta} &= (1 - \theta)U_i^n + \theta U_i^{n+1} \end{aligned} \quad (25)$$

At each point i the first and second spatial derivatives are approximated through centred differences and the time derivatives are approximated using forward differences.

The third equation of (25) is explicit relative to the r variable, and the resulting systems of equations for the first and fourth equations (h and U variables) are of three-diagonal form.

3.3. Finite elements method

The finite elements method is based on the approach of well-behaved functions. In the present case these are the water-depth

and the mean-averaged velocity, which are defined over small regions of finite dimensions (called finite elements) into which the problem domain is subdivided. Considering a generic element Δ^e , the functions h and U are approximated within each element by:

$$h \approx \hat{h} = \sum_{i=1}^n N_i h_i; \quad U \approx \hat{U} = \sum_{i=1}^n N_i U_i \quad (26)$$

where h_i and U_i represent the values of the functions h and U at the nodes of the element Δ^e , with n being the number of nodes of the element and N_i the interpolation (shape) functions, usually polynomials.

In accordance with the weighted residual technique, the residuals R_j (J varying between 1 and 3) are constructed first, by substituting the approximate values of the variables (\hat{h} and \hat{U}) in the above equation system (24).

According to the Galerkin method, minimization requires the ‘orthogonality’ of the residuals R_j to a set of weighting functions W_j , i.e.

$$\int_{\Delta^e} R_j W_j d\Delta^e = 0 \quad (27)$$

where $W_j = N_i \delta \phi_i$, $i = 1, \dots, n$.

To illustrate this procedure, a detailed solution of the continuity equation is presented here. The residual R_1 error minimization leads to the following Eq. (28):

$$\begin{aligned} \int_{\Delta^e} R_1 W_1 d\Delta^e &= \int_{\Delta^e} R_1 N_i \delta \phi_i d\Delta^e = \int_{\Delta^e} \left(\frac{\partial \hat{h}}{\partial t} + \hat{h} \frac{\partial \hat{U}}{\partial X} + \hat{U} \frac{\partial \hat{h}}{\partial X} \right) N_i \delta \phi_i d\Delta^e \\ &= \int_{\Delta^e} N_i \left[\sum_{j=1}^n N_j \left(\frac{\partial h_j}{\partial t} \right) + \sum_{k=1}^n \left(\frac{\partial N_k}{\partial X} \right) U_k \sum_{j=1}^n N_j h_j \right. \\ &\quad \left. + \sum_{k=1}^n N_k U_k \sum_{j=1}^n \left(\frac{\partial N_j}{\partial X} \right) h_j \right] d\Delta^e = 0 \end{aligned} \quad (28)$$

This equation may be written in matrix form as follows:

$$[A] \frac{\partial h}{\partial t} + [B] h = 0 \quad (29)$$

where matrix A and vector B elements are given by:

$$\begin{aligned} a_{i,j} &= \int_{\Delta^e} N_i N_j d\Delta^e; \quad i, j = 1, \dots, n \\ b_{i,j} &= \int_{\Delta^e} N_k U_k N_i \left(\frac{\partial N_j}{\partial X} \right) d\Delta^e \\ &\quad + \int_{\Delta^e} \left(\frac{\partial N_k}{\partial X} \right) U_k N_i N_j d\Delta^e; \quad i, j, k = 1, \dots, n \end{aligned} \quad (30)$$

The solution of equation system (29) provides the values of the nodal unknowns h_i . It may be solved using the following form:

$$\left(\frac{1}{\theta \Delta t} A^t + B^t \right) h^{t+\Delta t} = \frac{1}{\theta \Delta t} A^t h^t - \frac{1-\theta}{\theta} B^t h^t \quad (31)$$

with $0.5 \leq \theta < 1.0$.

The resulting matrix, although unsymmetrical, is in general very sparse.

A similar sequence of calculations is performed for the remaining residuals R_2 and R_3 , noting that the second derivatives can be reduced by using integration by parts (or Green’s theorem) [2].

4. Applications

The mathematical model expressed by the second approximation in σ^2 (system A – equation system (20)) has been solved numerically, as presented earlier.

As a first application of this model, Fig. 2a and b compare the results of a wave propagation, amplitude $a = 0.0124$ m, in a 0.10 m constant depth domain (horizontal plane bottom and with-

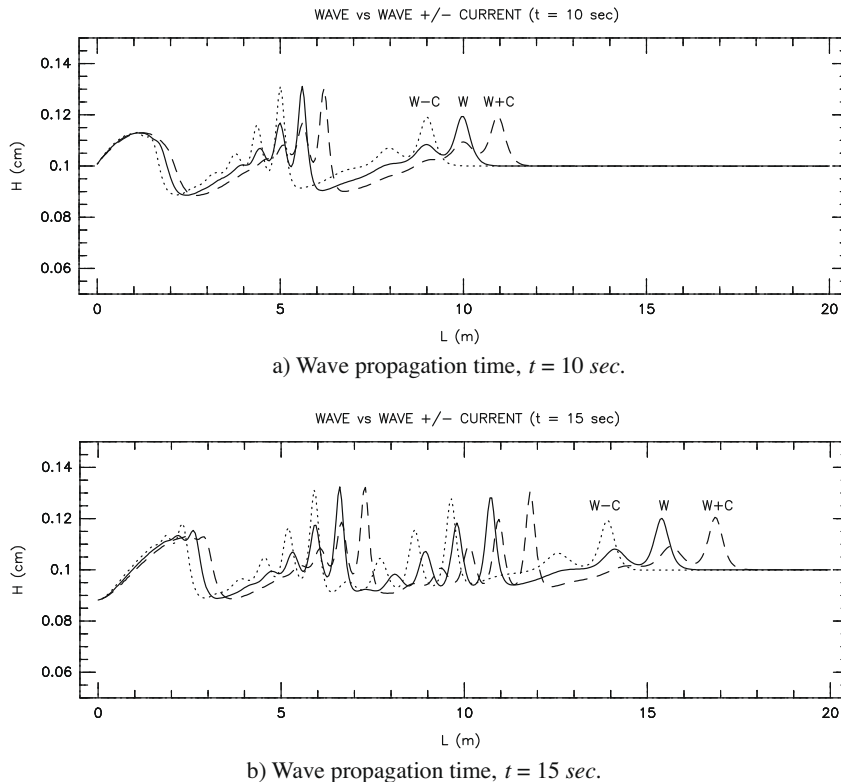


Fig. 2. Wave propagation over initial rest conditions (full line, W), wave propagation with a 0.10 m/s current (hatched line, W + C) and wave propagation against a 0.10 m/s current (dotted line, W – C).

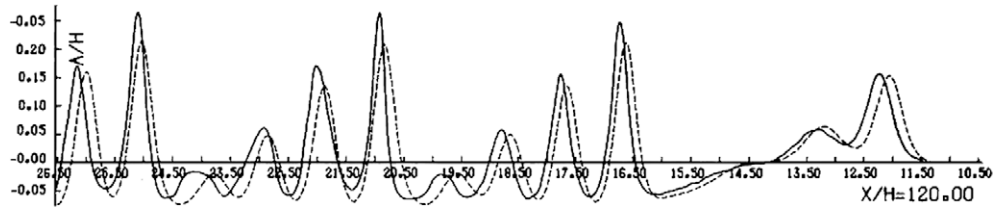
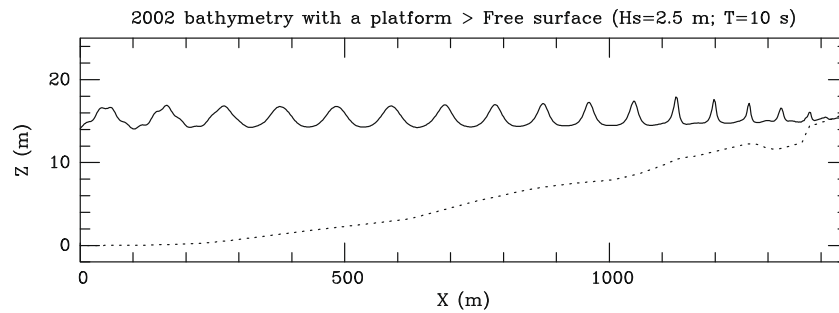
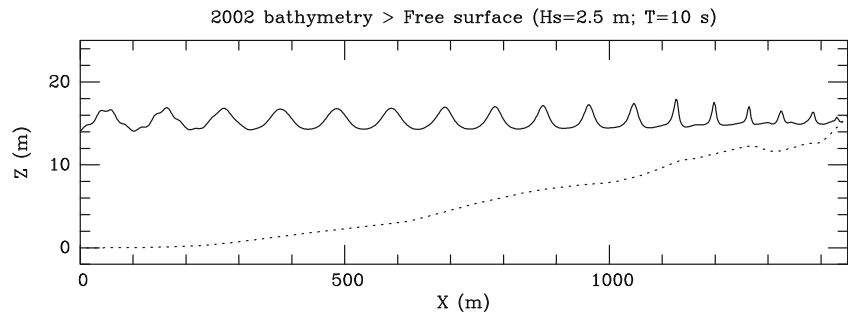
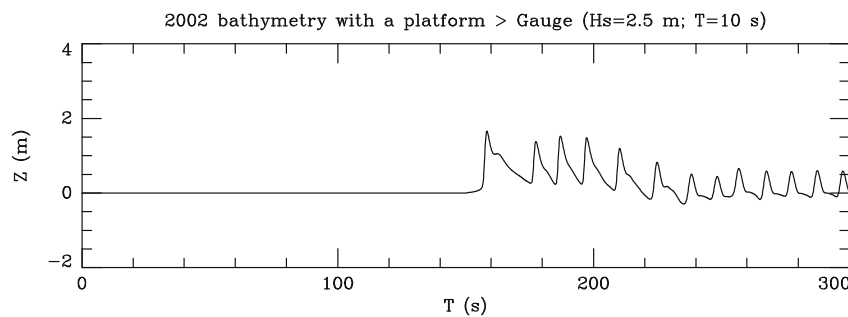
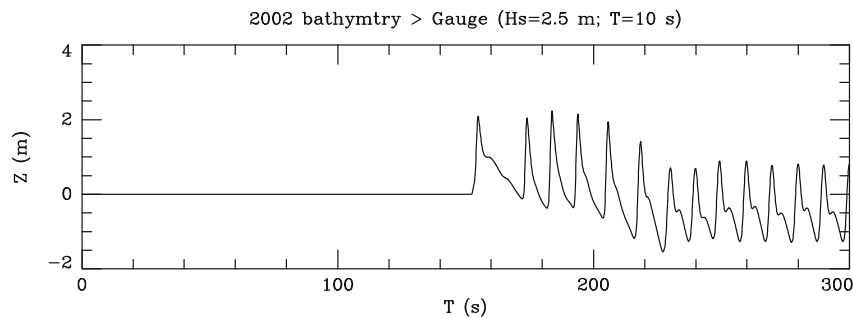


Fig. 3. Experimental data (continuous line) at a gauge placed 12 m from the input boundary (reproduced from [16]).



a) Numerical results obtained over the 2002 bathymetry and over a submerged platform in high-tide conditions (2002 bathymetry with a platform).



b) Numerical results in a gauge placed about 20 m from the sand dune base, considering the 2002 bathymetry and a constructed platform (2002 bathymetry with a submerged platform).

Fig. 4. Numerical results for a 2.5 m wave height propagation and 10.0 s characteristic period, in high-tide conditions (3.6 m above the HZ) [13,14].

out friction), for the times $t = 10$ s and $t = 15$ s, considering: initial rest conditions (W), a wave propagating with a 0.10 m/s current ($W+C$) and a wave propagating against a 0.10 m/s current ($W-C$), respectively.

Experimental results for the current alone are presented in Seabra-Santos et al. [16] and shown in Fig. 3. The comparisons between our numerical results and the experimental ones are very good in both space and time.

The second application consists of analysing and defining the characteristics of a wave dissipation energy structure, so its location and dimensions, with the purpose of protecting a sand dune severely damaged after the construction of an underwater effluent discharge channel. For details see Schreck Reis and Freitas [12], and Schreck Reis et al. [13,14].

As a consequence of the destruction occurring in February 2001, soft protection measures were considered insufficient and hard protection devices have been encouraged.

After various statistical studies based on observations and other information obtained by the ex-Autonomous Board of the Port of Figueira da Foz (Portugal) and by the Portuguese Hydrographic Institute, six typical situations were considered [4].

Two of them are presented here in detail, for significant wave heights of 2.5 m and 6.0 m, which correspond to wave periods of about 10 s and 15 s, respectively. These conditions represent characteristic situations of calms and storms, over a submerged structure with the crest level situated 2.0 m above the hydrographic zero (HZ) and tide heights of 3.6 m and 3.8 m above the HZ. Wave

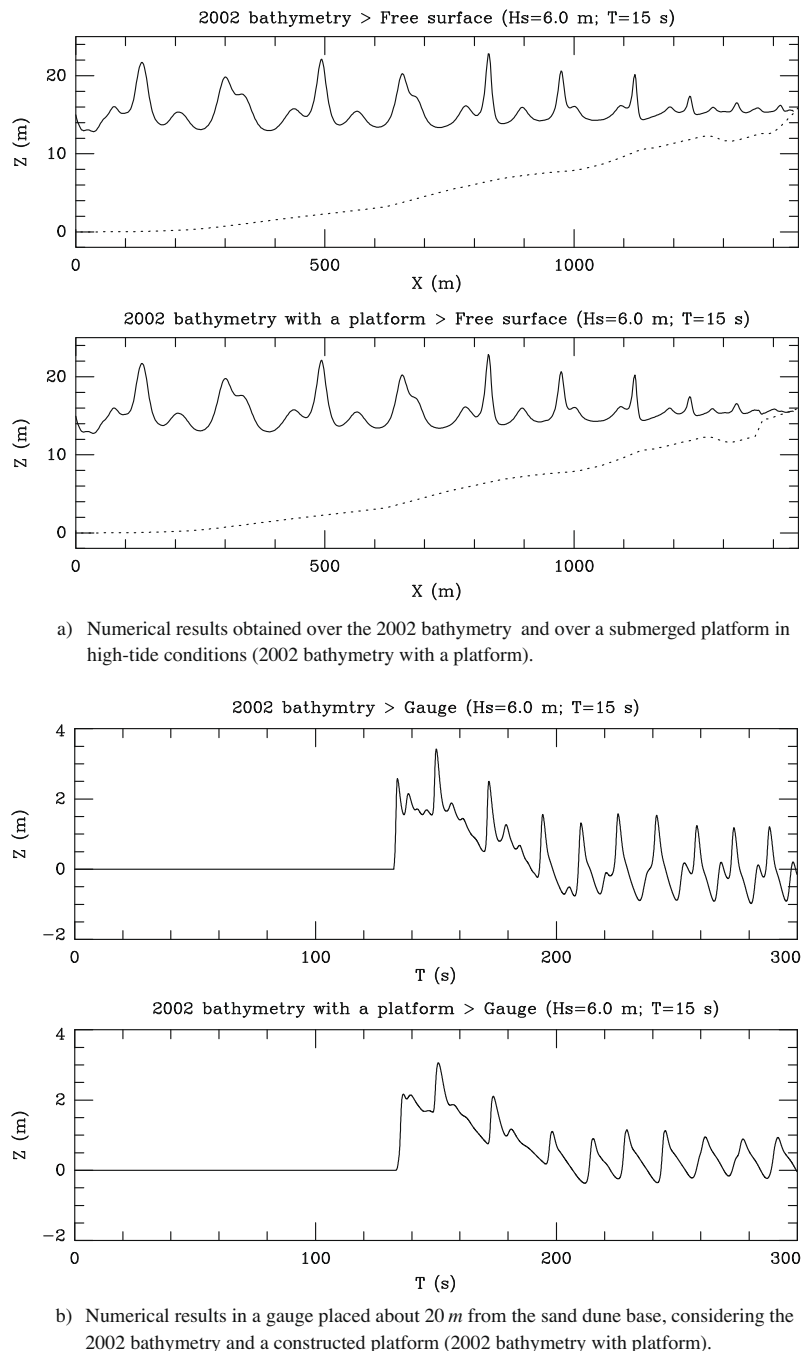


Fig. 5. Numerical results for a 6.0 m wave height propagation and 15.0 s characteristic period, in high-tide conditions (3.8 m above the HZ) [13,14].

breaking was simulated, as described in Antunes do Carmo and Seabra-Santos [2].

The results presented in Figs. 4 and 5 show the waves' behaviour over a bathymetry obtained in June 2002 [17]. These figures compare the numerical results obtained over that bathymetry without any platform installed (2002 bathymetry) with the results obtained over that bathymetry in high-tide conditions, with a submerged platform 70 m long and a 2.0–2.5% slope to the existing sand dune base (2002 bathymetry with a platform).

In order to determine the efficiency of the platform, we also give the results of a numerical gauge placed over the platform, about 20 m from the existing sand dune base, for the three selected simulations [13,14].

The above situations (Figs. 4 and 5) show a significant reduction of the wave amplitude and also, as a consequence, its energy potential, after the generalized wave breaking process over the platform, approximately 60–70 m away from the sand dune base and with a 2.0–2.5% slope.

Therefore, a submerged detached longitudinal structure, in high-tide conditions, with an approximate trapezoidal section, as presented in Fig. 6, was proposed. This structure was to be constructed from the bedrock, using stones of suitable weights and dimensions and having the crest level 2.0 m above the HZ.

For a better and deeper knowledge of the studies carried out on protecting the existing sand dune system see Schreck et al. [13,14].

A third application was tested, which consisted of generating and propagating a wave caused by a landslide moving into a reservoir. Fig. 7a and b show the experimental setup and the initial and final positions of a solid mass sliding into a reservoir over a bank with a 39.5° slope.

The reservoir is 12 m long and 0.55 m deep. Free surface variations were measured at gauges placed 2 m, 4 m, 6 m and 8 m

from the bank toe. For a better description of all experimental tests conducted in the hydraulics laboratory of the University of Coimbra's Civil Engineering Department see Carvalho and Antunes do Carmo [5].

The input boundary condition was obtained by video recording, depicting the sliding mass at times 0.16 s, 0.20 s, 0.36 s, 0.48 s, 0.52 s, 0.72 s, 0.96 s and the final position, at 1.08 s, after the complete stop of the solid mass on the reservoir bottom (Fig. 7b). Comparisons between the physical data and numerical results of a test case are shown in Fig. 8.

In spite of a slight loss of amplitude, particularly noticeable in the first wave (Fig. 8), the numerical results show an acceptable agreement with the experimental data.

5. Conclusions

Different mathematical and numerical formulations were developed, based on wave theory in shallow water conditions. It has been shown that the second approximation in order σ^2 can be employed to reproduce the flow in shallow water conditions, taking into account: (i) wave–wave and wave–current interaction effects; (ii) important ratios between the current and the wave velocities; (iii) appreciable bottom slopes and sudden time–bed-level changes, and (iv) friction stresses at the bottom and at the free surface.

The practical model applications presented in this work confirm the theoretical assumptions underlying its development.

As a first application, wave propagation under rest conditions, with a current and against a current shows that the model is able to reproduce the flow in shallow water conditions, with the wave–wave and the wave–current interactions.

The second application was a real world problem. The results obtained allow us to conclude that a submerged dissipation plat-

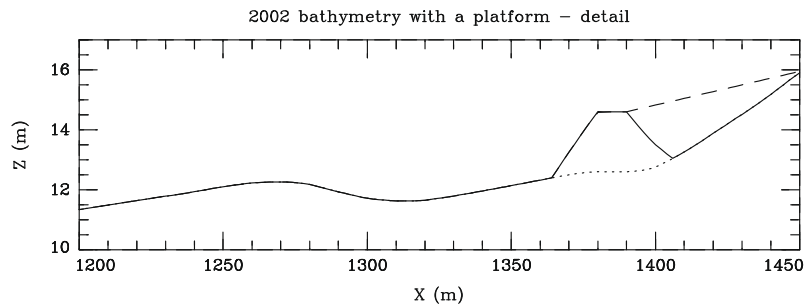


Fig. 6. Detail of the bathymetry with a platform installed (continuous line) 60–70 m before the existing sand dune base (at 1450 m – output boundary of the considered domain), with a 2.25% slope and crest situated 2.0 m above the HZ [13,14].

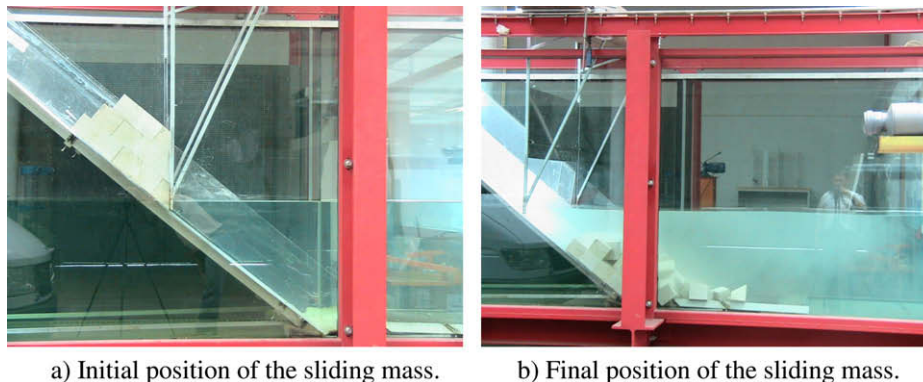


Fig. 7. Experimental setup: Initial (a) and final (b) positions of a solid mass sliding over a bank 39.5° slope into a reservoir 0.55 m deep.

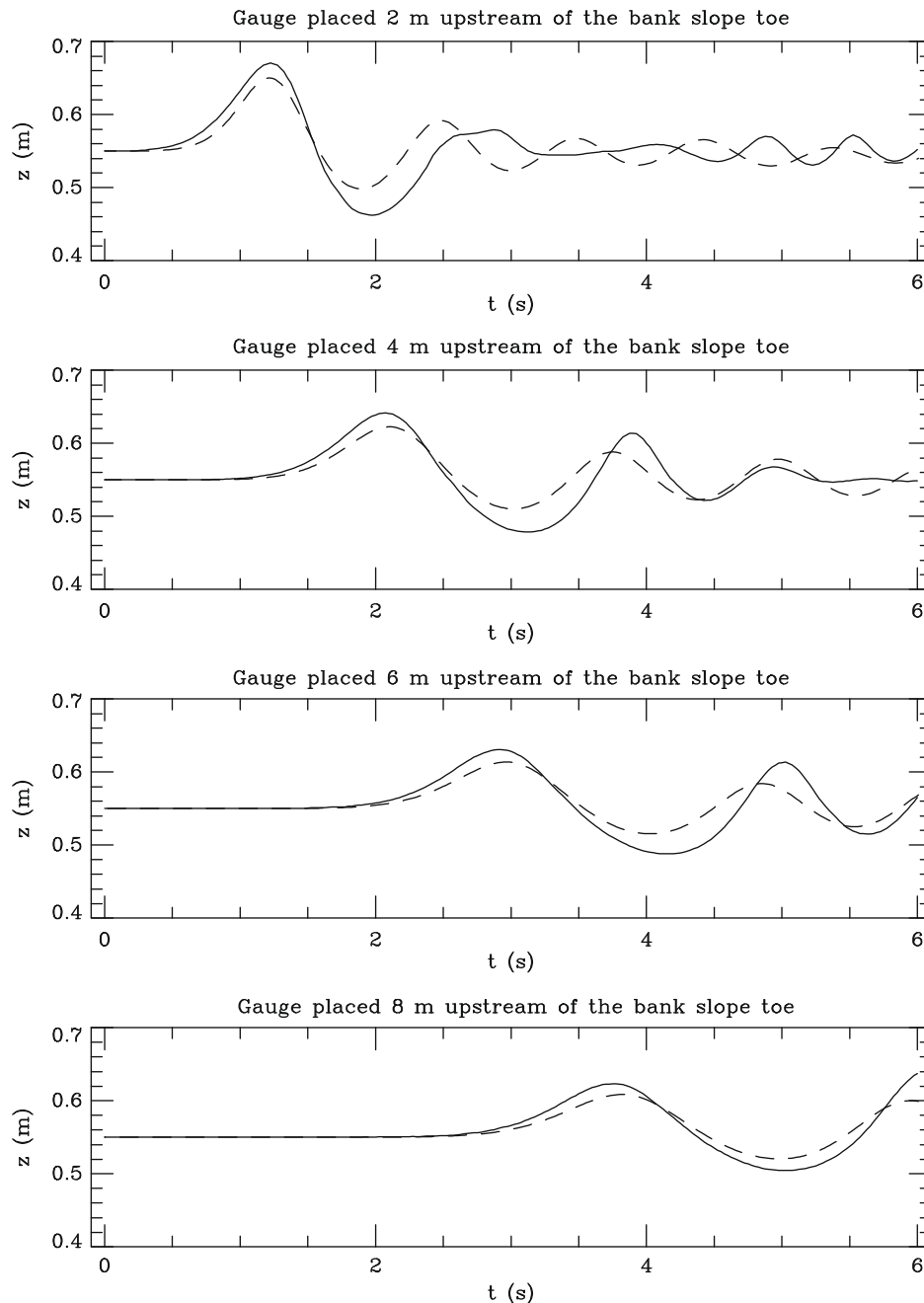


Fig. 8. Reservoir water level variations at 2 m, 4 m, 6 m and 8 m from the slide mass falling point. Comparisons of data obtained in the laboratory (continuous line) with numerical results.

form in high-tide conditions should be a good solution not only to resolve an existing coastal problem, but also to improve the bathing characteristics of a large coastal zone.

The third application was also a real world problem. It consisted of generating and propagating a wave resulting from a landslide moving into a reservoir. Various experiments were conducted in the laboratory, and the results of one were compared with the numerical results. In general we can say that the numerical results express the essential features of the phenomenon.

Therefore, the performance of the 1DH numerical model in the laboratory and in selected real-life cases is encouraging enough to proceed with further theoretical and physical comparisons having in view general real world 2DH applications.

Acknowledgement

The author wishes to acknowledge the Portuguese Foundation for Science and Technology for support under the Research Projects POCTI/ECM/2688/2003 and PTDC/ECM/66516/2006.

References

- [1] Antunes do Carmo JS, Seabra-Santos FJ, Barthélemy E. Surface waves propagation in shallow water: a finite element model. *Int J Numer Method Fluids* 1993;16:447–59.
- [2] Antunes do Carmo JS, Seabra-Santos FJ. On breaking waves and wave-current interaction in shallow water: a 2DH finite element model. *Int J Numer Method Fluids* 1996;22:429–44.
- [3] Antunes do Carmo JS, Seabra-Santos FJ, Amado-Mendes P. Sudden bed changes and wave-current interactions in coastal regions. *J Adv Eng Softw Elsevier Sci* 2002;33(2):97–107.

- [4] Antunes do Carmo JS. Littoral dynamics and coastal protection. A case-study. In: Proceedings of VI SILUSBA – hydraulics and water resources symposium that have Portuguese as the Official Language, Praia, Cabo Verde, November 10–13; 2003 [in Portuguese].
- [5] Carvalho RF, Antunes do Carmo JS. Landslides into reservoirs and their impacts on banks. *J Environ Fluid Mech Springer Netherlands* 2007;7(6):481–93. ISSN 1567-7419.
- [6] Gobbi MF, Kirby JT, Wei G. A fully nonlinear Boussinesq model for surface waves part 2 Extension to $O(kh)$. *J Fluid Mech* 2000;405:181–210.
- [7] Liu PL-F. Model equations for wave propagation from deep to shallow water. In: Liu PL-F, editor. *Advances in coastal engineering*, vol. 1. World Scientific; 1994. p. 125–57.
- [8] Lynett P, Liu PL-F. A two-layer approach to water wave modeling. *Proc Roy Soc Lond A* 2004;460:2637–69.
- [9] Madsen PA, Sørensen OR. A new form of the Boussinesq equations with improved linear dispersion characteristics part 2 a slowly-varying bathymetry. *Coast Eng* 1992;18:183–204.
- [10] Mei CC. *The applied dynamics of ocean surface waves*. John Wiley & Sons. ISBN 0-471-06407-6; 1983
- [11] Nwogu O. Alternative form of Boussinesq equations for nearshore wave propagation. *J Waterw Port Coast Ocean Eng ASCE* 1993;119(6):618–38.
- [12] Schreck Reis C, Freitas H. Rehabilitation of the Leirosa sand dune. *Littoral* 2002. The changing coast. Portugal: EUROCOAST. ISBN 972-8558-09-0; 2002.
- [13] Schreck Reis C, Freitas H, Antunes do Carmo JS. Leirosa sand dunes: a case study on coastal protection. In: Guedes Soares, Garbatov, Fonseca, editors. *Proc IMAM 2005*, published in maritime transportation and exploitation of ocean and coastal resources, Taylor & Francis Group, London. ISBN 0 415 39036 2; 2005.
- [14] Schreck Reis C, Antunes do Carmo JS, Freitas H. Learning with nature a sand dune system case study (Portugal). *J Coast Res* 2008;24(6):1505–15.
- [15] Seabra-Santos FJ. Contribution à l'étude des ondes de gravité bidimensionnelles en eau peu profonde. PhD thesis, Université Scientifique et Médicale et Institut National Polytechnique de Grenoble, Grenoble – France (in French); 1985.
- [16] Seabra-Santos FJ, Renouard DP, Temperville AM. Etude théorique et expérimentale des domaines de validité des théories d'évolution des ondes en eau peu profonde. *Annal Geophys* 1988;6(6):671–80 [in French].
- [17] StoraEnso. Dune erosion – sent data. Personal documentation offered by StoraEnso; May 2003.
- [18] Wei G, Kirby JT, Grilli ST, Subramanya R. A fully nonlinear Boussinesq model for surface waves part 1 highly nonlinear unsteady waves. *J Fluid Mech* 1995;294:71–92.
- [19] Zou ZL, Fang KL. Alternative forms of the higher-order Boussinesq equations: derivations and validations. *Coast Eng* 2008;55:506–21.